JOURNAL OF MATERIALS SCIENCE **38** (2003) 1747–1754

Modelling of static recrystallisation by the combination of empirical models with the finite element method

T. SHEPPARD, X. DUAN
DEC, Bournemouth University, 12 Christchurch Road, Bournemouth, UK BH1 3NA
E-mail: tsheppar@bournemouth.ac.uk

After rolling of aluminium alloys, static recrystallisation can modify product properties. The variation of properties throughout the stock thickness is of special interest to the producer. Predicting the recrystallisation kinetics by the combination of finite element method (FEM) with the various metallurgical models has attracted tremendous interest in both academia and industry. However, controversial results on the through-thickness distribution of the recrystallisation kinematics have been reported. The present paper attempts to explain this phenomenon from the viewpoint of the recrystallisation mechanism: the total stored energy, the growth rate of recrystallised grains, the Zener Hollomon parameter and the distribution of the equivalent strain. To improve the prediction accuracy, some new approaches are proposed on the calculation of equivalent strain and the Zener-Hollomon parameter. Some aspects related to the experimental establishment of these models are also critiqued.

1. Introduction

Modelling microstructural evolution during hot flat rolling of aluminium alloys has become increasingly important in the quest to improve final product properties. The deformation is applied in a series of passes, which are necessarily separated by periods of time. Microstructural changes may take place in this interpass time because the substructures produced by deformation are thermodynamically unstable. Static recovery and static recrystallisation (SRX) are two mechanisms which cause interpass microstructural changes. Compared with static recovery, SRX has a marked softening effect and is easily observed. SRX may have a significant influence on the rolling process. At the macro-level, it affects the rolling load and hence power through changing the flow stress of the stock. Accurate prediction of rolling load is of paramount importance to ensure a high standard strip profile, whilst the accurate calculation of power ensures the maximum productivity. At the micro-level, SRX influences the grain size, and hence the mechanical properties.

Two types of model exist: bulk empirical and so called physical models [1–3], which deal with the kinetics of SRX. Each model has its advantages. In general, empirical models are easy to use and have been partially accepted by industry for off-line microstructural control. The physical model is based on crystal plasticity and hence more attractive to the scientist. It does, however, require significant tuning of unknown constants. However, the physical models reveal the mechanics driving the transformation. It thus must represent the direction of future research.

Excellent reviews on modelling of SRX have been given by Gottstein *et al.* [4–5] and Shercliff Lovatt [6]. These are not repeated here. Only the approach: the combination between FEM and empirical model, is described in the present work. The relationship between the volume fraction recrystallised (X_V) and the holding time (t) is generally represented by Johnson-Mehl [7]-Avrami [8]-Kolmogorov [9] equation (JMAK):

$$X_V = 1 - \exp\left\{-0.693\left(\frac{t}{t_{0.5}}\right)^k\right\} \tag{1}$$

$t_{0.5}$ is the time to 50% recrystallisation, k is a constant. For three dimensional grain growth, the theoretical value is either 3 (site saturated nucleation) or 4 (constant nucleation). Experimentally, it is found to be close to 2. More useful discussion on the k value can be found in the literature [10].

$t_{0.5}$ is empirically expressed by

$$t_{0.5} = Ad_0^a \bar{\varepsilon}^b Z^c \exp\left(\frac{Q_{\text{rex}}}{GT_a}\right) \tag{2}$$

A, a, b, c are constants regressed from experimental data. It has long been recognised that the fraction recrystallised increases with decrease of the initial grain size (d_0), and with increase of Z (higher strain rate or lower deformation temperature), equivalent strain ($\bar{\varepsilon}$) and the annealing temperature (T_a). Hence a has a positive value; b and c have negative values. Q_{rex} and G in Equation 2 are the activation energy for recrystallisation

and the universal gas constant respectively. The Zener Hollomon parameter, Z, is defined by

$$Z = \dot{\bar{\varepsilon}} \exp\left(\frac{Q_{\text{def}}}{GT}\right) \tag{3}$$

where $\dot{\bar{\varepsilon}}$ is the mean equivalent strain rate, Q_{def} is the activation energy for deformation, T is the deformation temperature in degree Kelvin.

When using the empirical model, the FEA results are postprocessed to produce a mean value of Z and final equivalent strain for the differing through-thickness locations. These two values are then substituted into Equation 2 to derive the value of $t_{0.5}$, and finally the fraction recrystallised X_V is calculated by the use of Equation 1. Several attempts have been carried out by using this approach [11, 1, 2, 13, 19, 20] and all assumed plane strain deformation.

For the modelling of SRX after single pass deformation, Chen *et al*. [11] simply incorporated the FE output into Equation 2 without any modification, and their prediction were not validated by experimental or industrial data. The predicted fraction recrystallised fell from the surface to the centre. McLaren and Sellars [12] presented an unusual measurement of the fraction recrystallised through the stock thickness, see Fig. 1. The measured fraction recrystallised at the surface was smaller than that at the centre. Dauda and McLaren [13] measured and simulated the gradient of fraction recrystallised for high purity Al-3%Mg alloy. The measured rate of recrystallisation increased from the slab centre (3%) to the surface (15%). Their prediction is, however, much greater than the measurement at the surface. Yiu *et al.*'s measurement provided further quantitative evidence that the fraction recrystallised should fall from the surface to the centre see Fig. 2 [14].

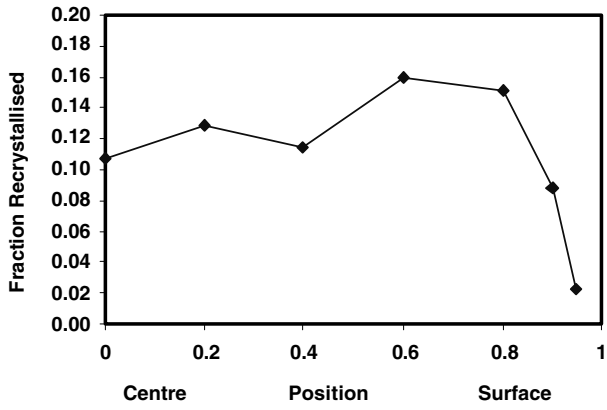

Figure 1 Measured gradients in fraction recrystallised [12].

In recent years, Nes *et al.* [15, 16] have proposed some physical models to calculate the recrystallisation kinematics. The models are based on three factors: the total stored energy, the mobility of grain boundary migration and the various nucleation sites. A major contribution in this field is due to these models which incorporate three possible nucleation sites: particle stimulated sites (PSN), nucleation at cube bands and nucleation at grain boundaries. Vatne *et al.* [17] have integrated the above physical model into a FEM code to predict the recrystallisation kinematics after a single pass rolling of AA3104. The predicted results also show that the fraction recrystallised at 12% depth (0 corresponding to the surface) is greater than that at 42% depth and the predicted recrystallised grain size is smaller at 12% depth than at 42% depth.

When modelling multipass hot flat rolling, Brand *et al.* predicted the grain size evolution for AA2024 during a 6-pass rolling schedule [18]. Their method to deal with the combination between FEM and empirical models seems efficient. But regretfully, they did not give the predicted distribution of the fraction recrystallised or any measured data of grain size or the fraction recrystallised. Their results show a small region near the surface where the grain is coarser than at the centre. Their conclusions were that " the kinetics for static recrystallisation is not evaluated exactly, the onset of SRX is calculated to occur too early in the multistage rolling process." Most recently, Mirza *et al.* reported a very small prediction of the fraction recrystallised at the surface and relative high prediction at the centre for a 17-pass industrial schedule for AA3104 using two different approaches [19]. No comparison with the measurement was presented in their work. In contrast, Wells *et al.* measured a slightly finer grain size at the surface than at the centre after 3-pass hot tandem rolling of AA5182 [20]. There is an obvious difference in the distribution of the predicted recrystallised grain size through the thickness. Black *et al.*'s micrographs provide further metallurgical evidence that rapid

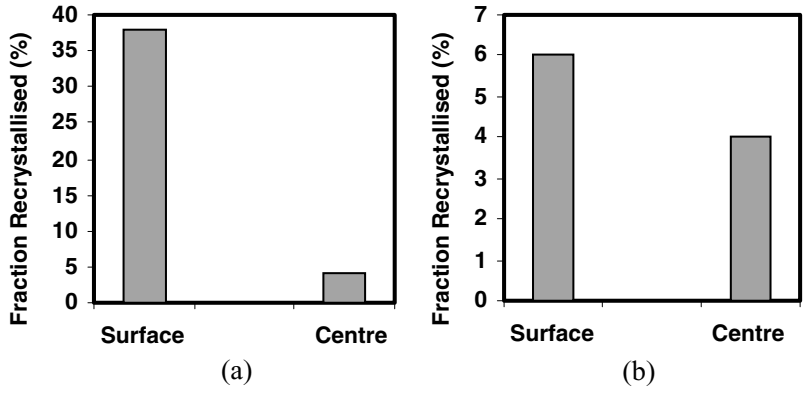

Figure 2 Comparison of fraction recrystallised (a) 4.45% Mg alloy and (b) 1% Mg alloy [14].

recrystallisation occurs at the surface in laboratory rolling [21].

All previous work on the observation and modelling of SRX has proved to be very confusing in several aspects either for single pass rolling or for multi-pass rolling. It indicates the complication of SRX. If we assume all previous measurements to be correct, we must explain the controversial results on the through-thickness distribution of the fraction recrystallised. The present paper discusses this phenomenon from three aspects: the total stored energy, the growth rate of the recrystallised grains and the Zener Hollomon parameter.

Strictly speaking, the mechanism of SRX has been studied and various models have been proposed. However, there are so many uncertain parameters within those models and these parameters are not easily determined by the current experimental techniques. Hence modelling of SRX is difficult because of the tuning required for the unknown constants.

From the above literature review, one conclusion can certainly be drawn: the fraction recrystallised is over-predicted at the surface region after a single pass deformation when FEM is applied in conjunction with empirical models. In the present paper, some new approaches are proposed to reduce this trend. The study is carried out from four aspects: the calculation of equivalent strain; the calculation of Z; averaging Z and the application of different empirical models.

2. Calculation of equivalent strain

In the calculation of equivalent strain used in Equation 2, four different methods have been proposed by McLaren and Sellars [12] in summing the strain components for plane strain deformation. Two definitions of equivalent strain are used in the present study:

Strain 1

$$\bar{\varepsilon} = \int \sqrt{\frac{2}{3}} \sqrt{\dot{\varepsilon}_x^2 + \dot{\varepsilon}_y^2 + 2\dot{\varepsilon}_{xy}^2}\, \mathrm{d}t \tag{4}$$

Strain 2

$$\bar{\varepsilon} = \int \sqrt{\frac{2}{3}} \sqrt{\dot{\varepsilon}_x^2 + \dot{\varepsilon}_y^2}\, \mathrm{d}t \tag{5}$$

In Equation 5, the contribution of the shear strain to the total accumulated equivalent strain is ignored. McLaren and Sellars [12] have demonstrated clearly that "accumulated equivalent strain by summing squares of components during deformation may give grossly erroneous results if these strains are applied in equations such as (2) for recrystallisation kinetics. The accumulation of shear strains irrespective of sign appears to be incorrect in regions where significant reversals in the direction of shear occur during rolling."

Dauda and McLaren adopted another definition of equivalent strain in their study [13]

$$\bar{\varepsilon} = \sqrt{\frac{2}{3}\varepsilon_{ij}\varepsilon_{ij}} \tag{6}$$

However, extra caution must be taken when using Equation 6 since it is proposed for small deformations. Hot rolling is typically a large deformation process, except for the first few passes in the hot breakdown rolling. To reduce the possible error introduced by the use of Equation 6 in FEM, the increments of time must be set at very small values to ensure a small deformation during each increment.

3. Calculation of Zener Hollomon parameter

Presently, there are two ways to calculate the value of Z for each node in FEM computation. The first method is simply substituting the nodal strain rate and nodal temperature into Equation 3 to calculate the history of Z. The Zener-Hollomon parameter calculated in this way is termed "instantaneous Zener-Hollomon parameter," represented by Z_{ins}, in this paper. The second method is using the averaged strain rate and nodal temperature to derive the value of Z. The Z calculated in this way is termed "averaged Zener-Hollomon parameter," represented by Z_{ave}. The averaged strain rate is obtained by averaging the strain rate over the whole deformation zone in each increment during the finite element computation. Adopting such an average strategy is logical since the strain rate in Equation 3, which is regressed from experimental data, is also a mean value over the whole deformation zone. Thus, in each increment during the finite element computation, all nodes have the same strain rate. The gradient of Z depends upon the gradient of temperature. According to the study conducted by Well *et al.* [20], temperature plays an overwhelming effect on determining the microstructure when compared with roll speed (strain rate), work roll temperature, and the friction coefficient. Hence, averaging strain rate over the whole deformation appears to be acceptable.

4. Averaging *Z*

As reported by Dauda and McLaren [13], the mean value of Z can be obtained by averaging the history of Z on the basis of time or strain. For Z_{ins}, the averaged value on the basis of increments of time and strain are given in Equations 7 and 8 respectively:

$$(\bar{Z}_{\mathrm{ins}})_t = \frac{\sum Z_{\mathrm{ins}} \Delta t}{t} \tag{7}$$

$$(\bar{Z}_{\mathrm{ins}})_\varepsilon = \frac{\sum Z_{\mathrm{ins}} \Delta \bar{\varepsilon}}{\bar{\varepsilon}} \tag{8}$$

where Δt and $\Delta\varepsilon$ are time and strain increments respectively, t is the total deformation time, $\bar{\varepsilon}$ is the final equivalent strain. For the Z_{ave}, similar definitions are given by:

$$(\bar{Z}_{\mathrm{ave}})_t = \frac{\sum Z_{\mathrm{ave}} \Delta t}{t} \tag{9}$$

$$(\bar{Z}_{\mathrm{ave}})_\varepsilon = \frac{\sum Z_{\mathrm{ave}} \Delta \bar{\varepsilon}}{\bar{\varepsilon}} \tag{10}$$

5. Finite element analysis model

This study is to improve prediction through introducing new approaches for the analysis of the FEM results and using recently proposed SRX models. The analysis model is taken from McLaren and Sellars's experiments [12, 22]. The material, commercial purity aluminium, is rolled with an initial temperature of 400°C in a single stand mill with roll diameter of 68 mm. The roll peripheral speed is 0.21 m/s. The initial slab thickness is reduced from 50 mm to 38 mm. After rolling, the specimen is water quenched. The specimen is annealed at 400°C, and the fractions recrystallised are measured after annealing for 426 seconds. The trace alloying elements in this material are 0.11%Si, 0.2%Fe, 0.001%Cu, 0.004%Mn, 0.002%Cr, 0.002%Zn and 0.013% Ti.

A commercial FEM program, FORGE2® V2.9.04 is employed. A plane strain deformation model is used to simulate the rolling process because the measurement of the fraction recrystallised was taken at the slab centre. Sticking friction is assumed in the finite element computation. The effective heat transfer coefficient between the roll and the slab is 25 kW m^{-2} K^{-1}, which is obtained by comparing the computed temperature history with the measured values taken from McLaren's work [22]. The material behaviour is described by the following constitutive equation:

$$\sigma = K\dot{\varepsilon}^{m_1}\exp(m_2 T)\,\varepsilon^{m_3}\exp(m_4/\varepsilon) \qquad (11)$$

where ε is the strain, $\dot{\varepsilon}$ is the strain rate, T is the temperature in degree Celsius, and K and m_1–m_4 are material dependent constants.

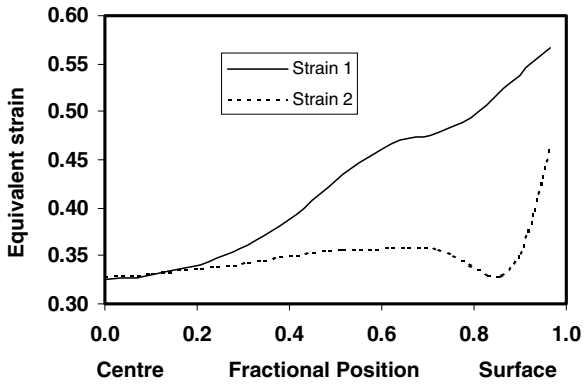

Figure 3 Variation of strain throughout the thickness. Strain 1 is defined by Equation 4; Strain 2 is defined by Equation 5.

6. Results and discussion

The predicted through thickness variation of the accumulated strains defined in Equations 4 and 5 are shown in Fig. 3. The lines marked "Strain 1" and "Strain 2" give the same value at the slab centre, where the effect of shear strain is negligible. From the centre to the surface, the difference between these two curves diverge due to increase of the shear strain. "Strain 1" rises gradually from the centre to the surface. However, for the line marked "Strain 2," there is a steep rise near the surface. "Strain 1" is much greater than "Strain 2" at the surface. This implies that there is a large shear strain generated by the contacting friction force.

The computed profiles of $(Z_{\text{ins}})_t$ and $(Z_{\text{ave}})_t$ are shown in Fig. 4. There also exists a significant difference between these two curves in the surface region. The maximum value appears at the surface, and the value of $(Z_{\text{ins}})_t$ is much greater than the value of $(Z_{\text{ave}})_t$.

In Figs 3 and 4, the maximum values of equivalent strain and Z are all located at the surface. If we just consider the Equations 1 and 2, the highest rate of recrystallisation should appear at the surface because more stored energy for recrystallisation is produced at the surface due to the low temperature, high strain rate and high strain. The stored energy can be calculated by the following model [2]:

$$P_D = \frac{Gb^2}{10}\left[\rho_i\left(1-\ln\left(10b\rho_i^{1/2}\right)\right) + \frac{2\theta}{b\delta}\left(1+\ln\left(\frac{\theta_c}{\theta}\right)\right)\right] \qquad (12)$$

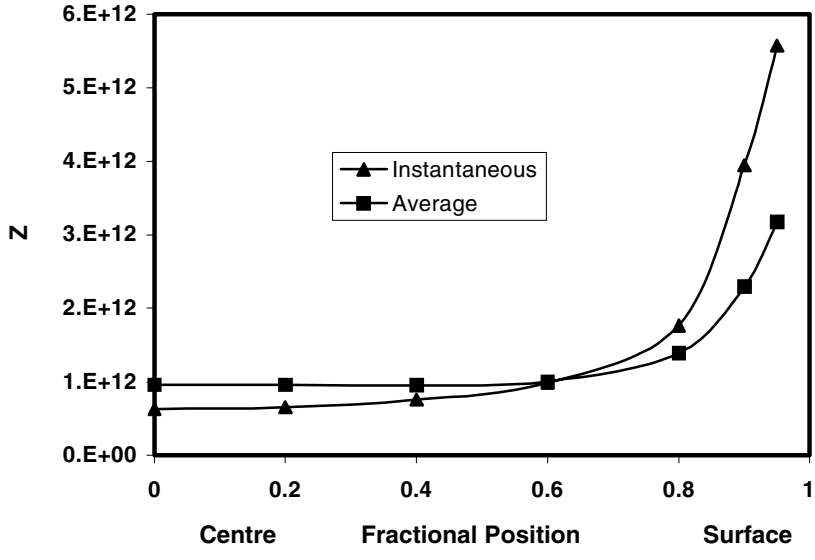

Figure 4 Comparison of the predicted gradients of the Zener-Hollomon parameter through the thickness, (Z_{ms}), and (Z_{ave}).

Figure 5 Distribution of the computed stored energy in Joules.

where G is shear modulus, b is the Burgers vector, ρ_i is the internal dislocation density, θ is misorientation, θ_c is the critical misorientation for high angle boundary, and δ is the subgrain size. The prediction of ρ_i, δ and θ by integrating FEM with physical models for hot flat rolling of aluminium alloys have been reported in the literature [23, 24]. The predicted distribution of the stored energy is given in Fig. 5. As expected we observe a decrease from the surface to the centre at exit.

If assuming site saturation and a random distribution of nucleation sites, for multi-pass rolling, the transformation kinetics law can be calculated by [15, 16]

$$X_n(t) = 1 - \exp\left[-X^n_{\text{ext}}(t)\right] \tag{13}$$

where $X_n(t)$ is the fraction recrystallised after nth pass after an inter-annealing time t and $X^n_{\text{ext}}(t)$ is the corresponding extended volume. $X^n_{\text{ext}}(t)$ is determined by

$$X^n_{\text{ext}}(t) = \frac{4}{3}\pi N^n_{\text{TOT}}(G_n t)^3 \tag{14}$$

N^n_{TOT} is the total number of nuclei after pass n. G_n is the growth rate of recrystallised grains, given by the following expression

$$G_n = M_n\left(P^n_D - P^n_Z\right) \tag{15}$$

where P_Z is the Zener drag term, M_n is the mobility. In the studies by Nes *et al.*, the mobility was assumed to be orientation independent and is calculated by

$$M_n = \frac{M_0}{kT_n}\exp\left(\frac{-U_{\text{GB}}}{kT_n}\right) \tag{16}$$

where M_0 and k are constants, and U_{GB} is the activation energy for grain boundary migration, which is a material constant. T_n is the temperature during the interpass annealing between nth and the $(n + 1)$th pass. For a single pass, T_n can be regarded as the annealing temperature.

Since it is very difficult to accurately determine the value of P_Z, Nes *et al.* assumed a constant in their calculation. It is clear that, from Equations 15 and 16, that the growth rate depends only on the total stored energy. The larger the total stored energy, the greater the growth rate. If we also assume the distribution of available nucleation sites is uniformly distributed through the thickness, models by Nes *et al.* supports the thesis that the fraction recrystallised should fall from the surface to the centre.

This does not explain the experimental observation by McLaren and Sellars. Some researchers consider that during recrystallisation, once a viable nucleus is formed, its growth is determined by the local driving pressure acting on the nucleus and by the mobility of the nucleus boundary. From Fig. 5 we already have concluded that the driving force decreases from the surface to the centre. The only possible interpretation is due to the fact that the mobility strongly depends on misorientation [25–27] and it was reported that "an increase in 3° results in a 50 times increase in mobility. The mobility of the low angle boundaries investigated were found to be some 10–500 times lower than the mobilities of random high angle boundaries and 100–5000 times lower than 40° ⟨111⟩ tilt boundaries" [25]. Sheppard and coworkers [28, 29] have found that the orientation of the grains within a small area below the roll/slab interface changes little before and after hot rolling due to the strong constraint applied by the sticking friction in laboratory experiments, whilst there is obvious grain rotation in the remaining area, especially around 20% depth. Hence the mobility within the small region below the roll/slab interface is much smaller, resulting in a small fraction recrystallised when compared with the centre.

The measured and calculated through thickness distributions of the fraction recrystallised under the conditions of annealing for 426 seconds is compared in Fig. 6 when Gutierrez *et al.*'s model [30] is applied with $(Z_{\text{ins}})_t$. Since the influence of the initial grain size on the kinetics of static recrystallisation is not included, Gutierrez *et al.*'s model has to be adjusted for

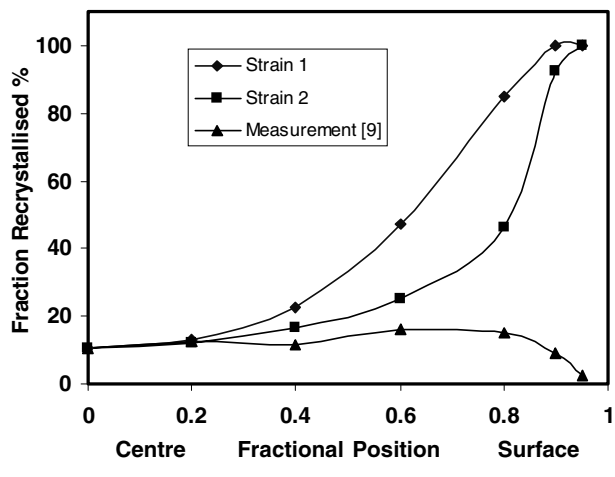

Figure 6 Comparison between the measured and the predicted gradients of the fraction recrystallised by using Gutierrez *et al.*'s model with $(Z_{\text{ins}})_t$.

the specific case. Here, Gutierrez *et al.*'s model is tuned on the basis of "Strain 1" by matching the predicted fraction recrystallised with the measurement at the slab centre. The tuned Gutierrez *et al.*'s model is expressed as

$$t_{0.5} = 1.45 \times 10^{-6} \varepsilon^{-1.5} Z^{-0.75} \exp\left(\frac{220000}{RT_a}\right) \quad (17)$$

This tuned equation is then applied for "Strain 2." It is clear from Fig. 6 that the measured fraction recrystallised drops to a very low value at the surface whereas the predicted lines give rapid recrystallisation in the surface region. Although the influence of shear strain is eliminated from "Strain 2," the prediction still can't match the measurement. This demonstrates that changing the definition of equivalent strain does not significantly improve the prediction of X_V in the surface region. Furthermore, tuning by altering the definition of $\bar{\varepsilon}$ is not really convincing. All the above analyses indicate the limitation of the empirical models.

The three reported single pass rolling conditions and measurements are shown in Table I. It is clear that Yiu *et al.*'s experiment is more close to industrial rolling than the other two experiments in terms of roll diameter, roll speed and rolling temperature. Comparing Dauda and McLaren and Yiu *et al.* measurements, it can be seen that the fraction recrystallised increases with increase of the percent of Mg and increase of reduction. As mentioned early, for commercial aluminium alloys, the number of nucleation sites and the stored energy are key for the occurrence of static recrystallisation. The number of nucleation sites depends upon the distribution of grain boundaries, dispersoids and precipitates, which are determined by the alloying elements and the substructure which is also a function of the alloy. In general, alloying elements tend to reduce the activation energy, making the movement of dislocations more difficult during deformation. The less the movement of dislocations, the more difficult it is for the occurrence of recovery and the easier it is for the occurrence of recrystallisation. The greater the reduction, the greater the stored energy becomes.

Fig. 7 shows the comparison in prediction by using $(Z_{\text{ins}})_t$ and $(Z_{\text{ins}})_\varepsilon$. The symbol "Strain 1-time" indicates that the corresponding curve is calculated by "Strain 1" and $(Z_{\text{ins}})_t$. The symbol "Strain 2-strain" indicates that the corresponding curve is calculated by "Strain 2" and $(Z_{\text{ins}})_\varepsilon$. It can be seen that averaging Z on the basis of strain appears to give a better prediction than that by averaging with time for both "Strain 1" and "Strain 2." This conclusion was also confirmed by Dauda and McLaren [13]. In the following computations, all Z, either Z_{ins} or Z_{ave}, are averaged with increments of strain.

TABLE I Comparison of the rolling conditions and measurement

	McLaren and Sellars [12]	Dauda and McLaren [13]	Yiu *et al.* [14]
Roll diameter (mm)	68	89	368
Rolling temperature (°C)	400	400	460
Relative reduction (%)	24	30	48
Roll peripheral speed (m/s)	210	200	385
% Mg in the alloy	<0.001	3	4.45 in Fig. 2a
Measured fraction recrystallised at the centre	10.7%	~3%	~6% in Fig. 2a
Measured fraction recrystallised at the surface	2.3%	~15%	~38% in Fig. 2a

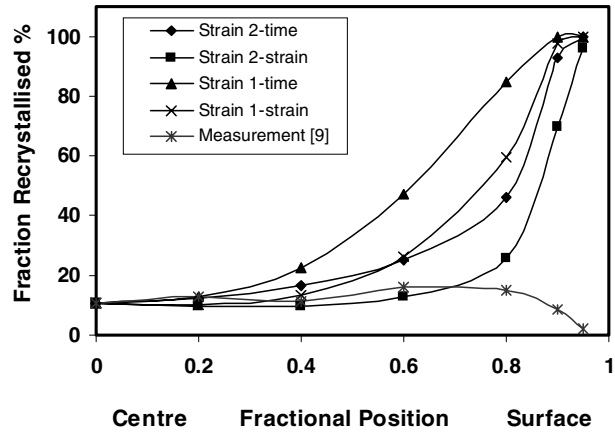

Figure 7 Comparison of the predicted profiles by using between (Z_{ins}) and $(Z_{\text{ins}})_\varepsilon$.

An alternative method to improve the prediction is a recently developed model by Liserre and Goncalves [31]. This model was modified from Gutierrez *et al.*'s model for commercial purity aluminium. Liserre and Goncalves's model is adjusted to "Strain 1" at the centre. The computed results are shown in Fig. 8. Unexpectedly, this model gives an irregular distribution of the fraction recrystallised through the thickness because the calculated values of $t_{0.5}$ is negative for some points on the lines. The error is introduced by the term "−6924" (See Appendix). Apparently, Liserre and Goncalves's model is basically in error.

Another method to decrease the difference between the prediction and the theoretical distribution is in modifying the mode of calculation for Z. "Averaged Zener-Hollomon parameter," Z_{ave}, defined in Section 3, will be applied. Fig. 9 shows the predicted profiles by using Gutierrez *et al.*'s model. Clearly, using Z_{ave} significantly improves the prediction for both strains.

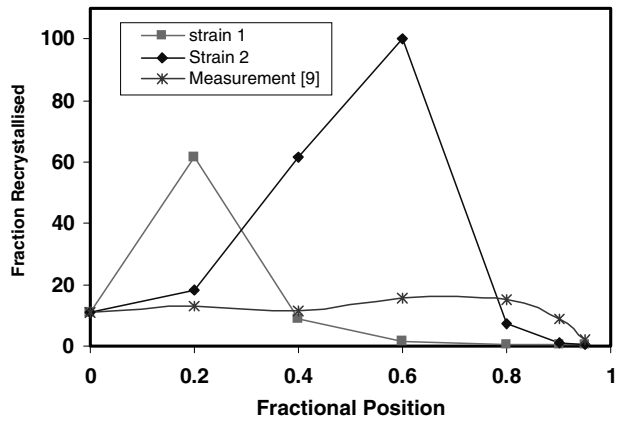

Figure 8 Comparison between the measured and predicted gradients of the fraction recrystallised by using Liserre *et al.*'s model with $(Z_{\text{ins}})_\varepsilon$.

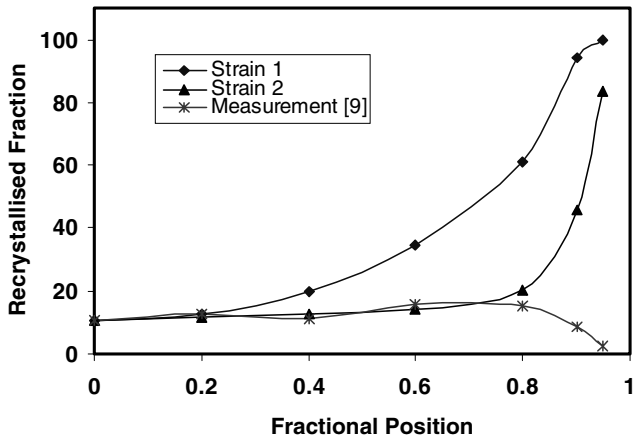

Figure 9 Comparison between the measured and predicted gradients in the recrystallised fraction by using Gutierrez *et al.*'s model with $(Z_{ave})_{\varepsilon}$.

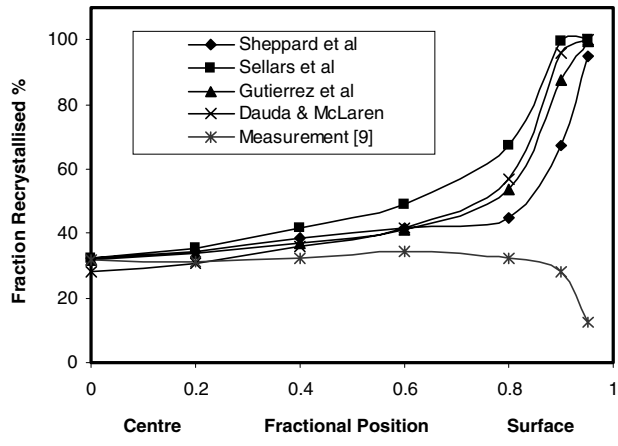

Figure 11 Comparison of the predicted gradients in the fraction recrystallised by using the different normalised models with the Strain 1 and $(Z_{ave})_{\varepsilon}$.

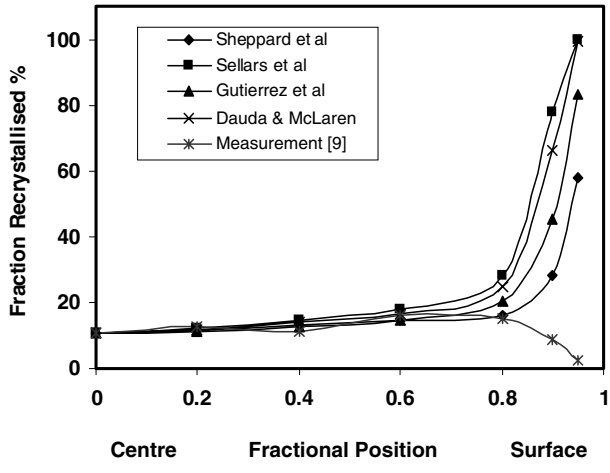

Figure 10 Comparison of the predicted gradients in the fraction recrystallised by using the different normalised models with the Strain 2 and $(Z_{ave})_{\varepsilon}$.

The comparison of various empirical models is shown in Fig. 10. These empirical models are all tuned with the measurement at the centre for "Strain 2." Contrary to expectation, the model established for commercial purity aluminium (Gutierrez *et al.*) does not give the best prediction for the rolling of commercial purity aluminium. The other three models provide nearly the same prediction within 70% thickness. Sheppard *et al.*'s model [32] proposed for aluminium alloy AA5056 gives the best agreement, particularly in the surface area. The predicted fraction recrystallised by using Sheppard *et al.*'s model is nearly half that predicted by using Sellars *et al.*'s model. This discrepancy with other models is of considerable importance because only Sheppard *et al.*'s models are regressed from rolling tests. The other three models are established either by plain strain compression (Sellars *et al.*'s model [33]) or the torsion test (Gutierrez *et al.* [30]).

In torsion testing, the effect of shear strain is dominant and shear strain does not change direction. The phenomenon that shear strain changes direction is not included. The magnitude of shear strain is much greater than those in plane strain compression (PSC) and rolling. In PSC, the magnitude of shear strain at the surface is lower than that in the rolling test where the slab is pulled into the roll gap by the net frictional force. Although there is a direction change at the contacting face in PSC testing, a specified material point at the interface only experiences uni-directional shear strains. Whilst in rolling, a specified material point at the surface first experiences a forward shear strain because its entering speed is lower than the roll peripheral speed. The surface shear strain disappears at the neutral point or neutral region. After that, the same material point experiences a backward shear strain. From the above comparison, it can be concluded that there is a considerable difference in the strain path between these testing methods. Black *et al.*'s work show that the strain path affects the static recrystallisation kinetics [21]. Rossi and Sellars [34] reported that PSC leads to faster kinetics of recrystallisation than rolling does by a factor of approximately 2.7. From the above discussion, it can be concluded that the empirical model should be established by the rolling test. Otherwise, the fraction recrystallised would be overpredicted.

Fig. 11 shows the results by using the "Strain 1," and $(Z_{ave})_{\varepsilon}$. It is clear that the model due to Sheppard *et al.* still give the better prediction. Comparing the curves presented in both Figs 10 and 11, it can be seen that all empirical models present the same kind of distribution: the X_V changes smoothly in most of the region through the thickness and there is a small area, at the surface, where the X_V varies greatly.

7. Conclusions

Most of previous work on the prediction of the fraction recrystallised by integrating empirical models (Equations 1 and 2) into the FEM code tends to overpredict at the surface region for both single pass rolling or multi-pass rolling. Some unusual results have been reported. But most would agree that the recrystallisation at the surface is great than at the centre. Based on the analysis from the viewpoint of the total stored energy, the mobility, the distribution of strain and Zener Hollomon parameter, the present paper concludes that most of the existing models for the calculation of the fraction recrystallised are inadequate because they do not account for strain path and the mobility.

Various alternatives have been investigated in the calculation of equivalent strain and the mean value of Z, and on the selection of different SRX models in order to reduce the predicted fraction recrystallised at the surface. Significant improvement has been achieved for the whole thickness by the use of "Strain 2," Z_{ave}, and averaging Z on the basis of increments of strain.

The predictions obtained by the use of various empirical models show that: the X_V changes smoothly through most of the thickness and there is a small area where the X_V varies greatly.

The simulation also shows that the empirical model should be constructed from rolling tests. When constructing an empirical model for a new material, we should not just modify the constant A but keeping the constants b and c in Equation 2 from existing models which were constructed for differing materials. Otherwise incorrect results will be given.

Alternatively, empirical models should be constructed using the actual strain, strain, rate and temperature path, especially from the area from which the measurements of X_V are taken.

Appendix: Various empirical models for the prediction of static recrystallisation

Gutierrez *et al.*'s equation [30]

$$t_{0.5} = 1.5 \times 10^{-4} \varepsilon^{-1.5} Z^{-0.75} \exp\left(\frac{220000}{RT_a}\right)$$

Liserre *et al.*'s equation [31]

$$t_{0.5} = 9.85 \times 10^{-6} \varepsilon^{-1.5} Z^{-0.75} \exp\left(\frac{220000}{RT_a}\right) - 6924$$

Dauda and McLaren's equation [13]

$$t_{0.5} = A\varepsilon^{-2.7} Z^{-1.1} \exp\left(\frac{205000}{RT_a}\right)$$

Sellars *et al.* equation [33]

$$t_{0.5} = 9.8 \times 10^{-6} d_0^{1.35} \varepsilon^{-2.7} Z^{-1.1} \exp\left(\frac{230000}{RT_a}\right)$$

Sheppard *et al.*'s equation for AA5056 [32]

$$t_{0.5} = 9.1 \times 10^{-12} d_0^{1.52} \left(0.0286 + 1.8\varepsilon^{1.52}\right)^{-1} Z^{-0.35} \times \exp\left(\frac{212000}{RT_a}\right)$$

References

1. E. NES, *Progress in Materials Science* **41** (1998) 129.
2. C. M. SELLARS and Q. ZHU. *Materials Science and Engineering* A **280**(1) (2000) 1.
3. M. GOERDELER and G. GOTTSTEIN, *Materials Science & Engineering* A **309/310** (2001) 377.
4. G. GOTTSTEIN, V. MARX and R. SEBALD, *J. Shanghai Jiaotong University* **E-5**(1) (2000) 49.
5. G. GOTTSTEIN, V. MARX and R. SEBALD, in "The Fourth Inter. Conf. On Recrystallisation and Related Phenomenoa" edited by T. Sakai and H. G. Suzuki (Japan, 1999) p. 15.
6. H. R. SHERCLIFF and A. M. LOVATT, *Phil. Tran. R. Soc. Lond.* A **357** (1999) 1621.
7. W. A. JOHNSON and R. F. MEHL, *Trans. AIME* **135** (1939) 416.
8. M. AVRAMI, *J. Chem. Phys.* **7** (1939) 1103.
9. A. N. KOLMOGOROV, *USSR Ser. Metemat.* **1** (1937) 355.
10. R. A. VANDERMEER and D. JUUL JENSEN, *Metallurgical and Materials Transactions* A **26A**, **9** (1995) 2227.
11. B. K. CHEN, P. F. THOMON and S. K. CHOI, *Materials Science and Technology* **8** (1992) 72.
12. A. MCLAREN and C. M. SELLARS, in "Strip Casting, Hot and Cold Working of Stainless Steels" edited by Ryan N. D. *et al.* (Met. Soc. CIM, Montreal, Canada, 1993) p. 107.
13. T. A. DAUDA and A. J. MCLAREN, in "Modelling of Metal Rolling Processes 3," edited by J. H. Beynon *et al.* (London, 1999) p. 257.
14. H. L. YIU *et al.*, in "Hot Deformation of Aluminum Alloys," edited by T. G. Langdon *et al.* (Detroit, 1999) p. 509.
15. E. NES and K. MARTHINSEN, Proc. in "Hot Deformation of Aluminium Alloys II," edited by T. R. Bieler *et al.* (TMS, Chicago, 1998) p. 171.
16. H. E. VATNE, T. FURU, R. ØRSUND and E. NES, *Acta Mater.* **44**(1) (1996) 4463.
17. H. E. VATNE, F. PEROCHEAU, H. E. EKSTR M, L. POIZAT, K. V. NORD, M. KNUT, E. LINDH, J. HAGSTR M and T. FURU, *Mater. Sci. Forum* **331–337** (2000) 551.
18. A. J. BRAND, S. KALZ and R. KOPP, *Comput. Mater. Sci.* **7** (1996) 242.
19. M. S. MIRZA, C. M. SELLARS, K. KARHAUSEN and P. EVANS, *Materials Science and Technology* **17** (2001) 874.
20. M. A. WELLS, D. J. LLOYD, I. V. SAMARASEKERA, J. K. BRIMACOMBE and E. B. HAWBOLT, *Metallurgical and Materials Transactions* B **29B** (1998) 709.
21. M. P. BLACK, R. L. HIGGINSON and C. M. SELLARS, *Materials Science and Technology* **17** (2001) 1055.
22. A. J. MCLAREN. PhD thesis, University of Sheffield, 1994.
23. X. DUAN and T. SHEPPARD, *Journal of Materials Processing Technology* **125/126** (2002) 181.
24. X. DUAN and T. SHEPPARD, *Computational Materials Science*, in press.
25. Y. HUANG and F. J. HUMPHREYS, *Acta Mater.* **48** (2000) 2017.
26. Y. HUANG and F. J. HUMPHREYS, *Acta Mater* **48** (1999) 2259.
27. D. J. JENSEN, M. T. LYTTLE and N. HANSEN, in "Hot Deformation of Aluminium Alloys II," edited by T. R. Bieler *et al.* (TMS, Chicago, 1998) p. 9.
28. M. A. ZAIDI and T. SHEPPARD, *Metal Sciences* **16** (1982) 229.
29. N. RAGHUNATHAN and T. SHEPPARD, *Materials Science and Technology* **5** (1989) 542.
30. I. GUTIERREZ *et al.*, *Materials Science and Engineering* A **102** (1988) 77.
31. G. LISERRE *et al.*, in "Sixth International Conference on Aluminium Alloys," edited by T. Sao *et al.* (Toyohashi, Japan, July 1998) p. 395.
32. T. SHEPPARD *et al.*, in "Microstructural Control in Aluminium Alloys: Deformation, Recovery and Recrystallization," New York, 27 Feb. 1985, edited by Chia, E. Henry and H. J. McQueen (The Metallurgical Society, Inc., New York, 1986) p. 19.
33. C. M. SELLARS *et al.*, in "Microstructural Control in Aluminium Alloys: Deformation, Recovery and Recrystallization." New York, 27 Feb. 1985, edited by C. E. Henry and H. J. McQueen (The Metallurgical Society, Inc., New York, 1986) p. 179.
34. P. L. ORSETTI ROSSI and C. M. SELLARS, *Materials Science Forum.* **217–222** (1996) 379.

Received 1 March 2002
and accepted 8 January 2003